Article

Study of the Efficiency of Layered Double Hydroxide-based Corrosion Inhibitors on Mild Steel in Chemical Pickling in HCl Medium

Ayoub Salim[1], Said Elharrari[1], Gregory Guilbert[2], Driss Lahem[2], Adnane Seman[4], Mohamed Anouar Harrad[4], Mohammed Badreddine[4], Ahmed Legrouri[3], Driss Takky[1] and Youssef Naimi[1,*]

[1] Laboratory of Chemistry and Physics of Materials, Ben M'Sik Faculty of Science, Hassan II University, Casablanca, Morocco
[2] Materia Nova asbl, Avenue Nicolas Copernic 3, B-7000 Mons, Belgium
[3] Al Akhawayn University, Ifrane 53000, Morocco, and International University of Grand-Bassam, BP 564, Grand Bassam, Côte d'Ivoire
[4] Centre Régional des Métiers de l'Education et de la Formation, CRMEF, Marrakech-Safi, Morocco
* Correspondence: youssefnaimi@outlook.com

Abstract: The materials used as corrosion inhibitors are [Zn-Al-Cl], [Mg-Al-Cl], [Ni-Fe-Cl], and [Co-Fe-Cl] layered double hydroxides (LDHs). They were synthesized by coprecipitation and characterized by X-ray diffraction (XRD), Fourier transforms infrared spectroscopy (FTIR), and thermal analyses. The efficiency of these corrosion inhibitors on mild steel in concentrated hydrochloric acid (18.5%) at 60°C (chemical pickling conditions of steel) was studied using electrochemical and gravimetric methods for different concentrations. The surface morphology and composition were examined by scanning electron microscopy (SEM) and energy dispersive spectroscopy (EDS), respectively. The inhibitory efficiency in the case of 1.2 $g.L^{-1}$ LDH was found to be 83.33%, 83.65%, 68.38%, and 74.73% for [Ni- Fe-Cl], [Zn-Al-Cl], [Co-Fe-Cl], and [Mg-Al-Cl], respectively.

Keywords: layered double hydroxides; corrosion inhibitor; hydrochloric acid; chemical pickling; mild steel

1. Introduction

Corrosion is the degradation of a material and its properties caused by a chemical or electrochemical reaction between the material and its environment [1]. Carbon steel is the most widely used alloy in the metallurgical industry because it offers many advantages. On one hand, it is less expensive relative to other alloys and, on the other, it has suitable mechanical characteristics [2–4]. Yet, a chemical pickling step is required in its industrialization process to eliminate metallic impurities and standardize its surface [5–10]. Hydrochloric acid (HCl) is one of the most widely used agents in the industry for steel pickling, cleaning, etc. [11]. However, this chemical is known to cause severe degradation of metals and metal alloys, either through chemical or electrochemical reactions. Fortunately, several protection measures can be used to inhibit the effects of corrosion, such as cathodic protection[12] , inhibitor additives [13], passivation [14], and protective coatings [15].

Chemical pickling consists of removing grease by chlorinated solvents and rust by acids (acid pickling). The main disadvantage of this method is the formation of gaseous hydrogen that tends to penetrate the metal and weakens it.

In order to slow or stop this corrosion process, some chemical inhibitors are added in low concentrations to the system [16–18]. The main role of the corrosion inhibitor in chemical pickling is to minimize the acid attack on the steel and to reduce the loss of mass during this operation [19,20]. Inhibitors are generally classified according to the nature of the electrochemical reactions they trigger [21,22]:

- Anodic inhibitor.
- Cathodic inhibitor.

Preprints (www.preprints.org) | NOT PEER-REVIEWED | Posted: 16 June 2023 doi:10.20944/preprints202306.1177.v1

• Mixed inhibitor: acting on both reactions.

They are also classified according to their mode of action:

• Absorption inhibitor.

• Passivating inhibitor.

Some solid materials have been extensively researched and used as corrosion inhibitors due to their excellent stability and efficiency. These substances are often applied to steel surfaces either as coatings or in solution. Metal oxides, which create a barrier on the surface of steel, like iron and zinc oxides, are among the most often employed solid inhibitors [23–25]. Other substances, like calcium carbonate and magnesium hydroxide, are also efficient inhibitors due to their capacity to neutralize acids [26]. Organic inhibitors, such as quaternary ammonium compounds and imidazolines, have proven to be extremely efficient in preventing corrosion due to their adsorption capacity on the steel surface and subsequent creation of a protective layer . Overall, a potential strategy for reducing corrosion and lengthening the lifespan of metal and alloy structures is the use of solid chemical compounds as corrosion inhibitors [27,28].

Among the corrosion inhibitors commonly used as electrolytes for industrial water treatment are numerous mineral substances such as chromates, molybdates, nitrites, sulfites, phosphates, and polyphosphates. However, their use is limited either for technical reasons, such as the hydrolysis temperature for polyphosphates, or for their toxicity , especially with regard to chromates and nitrites [29–31].

Layered double hydroxides (LDHs), also referred to as anionic clays, are compounds characterized by a two-dimensional structure formed by a stacking of brucite-type sheets in which part of the divalent metal cations are replaced by trivalent metal cations (Fig. 1). M^{2+} represents a divalent metal (Zn^{2+}, Mg^{2+}, Ni^{2+}, Fe^{2+}, Mn^{2+} ...), M^{3+} represents a trivalent metal (Al^{3+}, Fe^{3+}, Co^{3+}, Cr^{3+}, Mn^{3+} ...), A^{m-} is the compensating anion (Cl^-,NO^-, ClO^{2-}, CO^{2-}...), and n is the number of water molecules located in the interlamellar space with the anion [32–34]. The coefficient, x, is the M^{3+}/M^{2+} mole fraction.

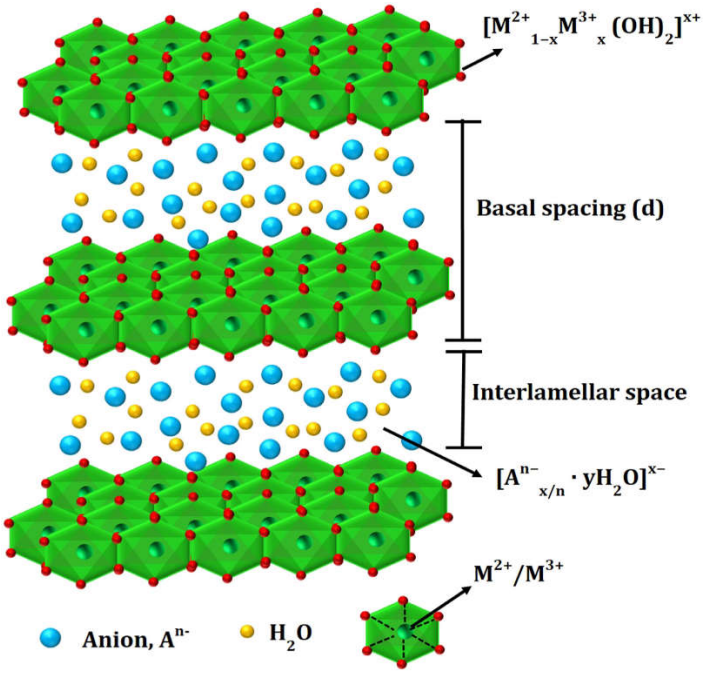

Figure 1. Structure of layered double hydroxides[35].

LDHs have many applications in industrial, medical, ecological and scientific fields due to their lamellar structure, varied compositions, ease of synthesis, low cost, low toxicity, significant anion exchange capacity, and redox or acid-base behavior [36–38] LDHs have recently attracted attention as corrosion inhibitors, as they offer exceptional corrosion prevention capability [39–42].

Preprints (www.preprints.org) | NOT PEER-REVIEWED | Posted: 16 June 2023 doi:10.20944/preprints202306.1177.v1

We propose in the context of this work to use [Zn-Al-Cl], [Mg-Al-Cl], [Ni-Fe-Cl], and [Co-Fe-Cl] LDHs as inhibitors in order to improve the electrochemical corrosion resistance of mild steel in HCl. Therefore, the steel plates were placed in the electrolytic solutions obtained by dissolving the LDHs in the corrosive environment. The inhibitory efficiency was determined by the gravimetric and electrochemical methods. The mode of the electrolyte action and certain corrosion parameters were identified.

2. Materials and methods

2.1. Preparation of the LDHs

The [Zn-Al-Cl], [Mg-Al-Cl], [Ni-Fe-Cl], and [Co-Al-Cl] LDHs were prepared by coprecipitation[43–46]. In a three-vial flask containing 250 mL of water, a mixture of 1 M MCl_2 and 1 M MCl_3 salts is added dropwise in a 2:1 molar ratio under moderate stirring. The pH of the solution was maintained at 9 by the addition of NaOH, using an automatic system. The coprecipitation is carried out under a nitrogen atmosphere to minimize the contamination by carbonate ions from the air. The precipitate obtained is left under moderate stirring at room temperature for 80 hours. The solid phase is obtained after repeated centrifugations and washings with demineralized water (4 times). It is then dried at room temperature (25°C). The materials were characterized by XRD, FTIR, and thermal analyses.

2.2. Steel Samples

The mild steel samples used in this study were polished before the experiments with various emery paper grades of 220, 400, and 800, rinsed with bi-distilled water, degreased with acetone, and then washed again with bi-distilled water. Finally, the samples were air-dried before use.

The chemical composition of the steel used (GRADD plate: DD13 from Maghreb Steel, Casablanca, Morocco) is given in Table 1.

Table 1. Chemical composition of the substrate steel used (GRADD plate: DD 13).

Element	Fe	Cu	C	Mn	Si	P	S	Ni	Cr	V
Weight percent (%)	99.41	0.2	0.04	0.18	0.025	0.02	0.015	0.03	0.03	0.05

2.3. Methods

The XRD equipment used was a Pert-Pro diffractometer (Bruker-AXS). Powder samples were exposed to copper Kα radiation (λ = 0.15415 nm).

IR spectra were recorded on a Perkin Elmer 16 PC spectrophotometer at a resolution of 2 cm^{-1} and averaging over 100 scans, in the range of 400 to 4000 cm^{-1}. The pellets consist of 100 mg of finely powdered KBr and 2 mg of the sample.

Thermal analyses were performed in air on a Setaram TG-DSC 92 instrument. Curves were recorded between 25 and 900°C at a heating rate of 5°C/min.

The surface morphology of the samples was examined by a Nikon optical microscope and Hitachi SU8020 SEM, coupled with an EDS.

2.4. Evaluation of inhibitory efficiency

The comparative study of the inhibiting efficiencies was achieved by gravimetry and linear voltammetry. The samples were immersed in an 18.5% HCl solution, in the absence and presence of the LDH-based inhibitor (1.2 $g.L^{-1}$). The samples were removed, rinsed, and dried before examination.

2.4.1. Gravimetric method

The test consists of stripping a sample of steel (area: S = 4 cm × 2 cm, thickness: e = 2.7 mm) in the HCl solution at 60°C followed by its immersing it in a mixture of the acid and the inhibitor at different LDH concentrations (C) ranging from 0 up to 1.2 $g.L^{-1}$. The LDH-based inhibitors used are

Preprints (www.preprints.org) | NOT PEER-REVIEWED | Posted: 16 June 2023 doi:10.20944/preprints202306.1177.v1

soluble under these acidic conditions. The steel-solution contact time is set for 10 min. The sample is then rinsed with demineralized water, dehydrated using filter paper, and dried in the oven at 100°C.

The mass variation of the sample is determined without (Δm_0) and with (Δm_f) the inhibitor. The inhibitory efficiency (IE) is calculated by the following formula:

$$IE = (\Delta m_0 - \Delta m_f)/\Delta m_0$$

2.4.2. Linear voltammetry

The linear voltammetry method, at low speed of potential sweep, allows to determine the kinetic parameters of the corrosion reaction of steel in the solution. The tests were performed at 60°C in an 18.5% HCl solution using a three-compartment cell with a platinum counter electrode and an Ag/AgCl electrode as a reference. The working electrode is a steel disc of 0.8 cm diameter.

The three electrodes are connected to an SP-150 Biologic potentiostat controlled by a computer via an "Ec-Lab" software. The corrosion potential covers the anodic and cathodic zones (- 0.350 to 0.350 V) at a scan rate of 2 mV/s. The inhibitory efficiency (IE) is calculated by the following formula. Where $I_{corr,0}$ and $I_{corr,f}$ are the corrosion current densities with and without inhibitor, respectively:

$$IE = (I_{corr,0} - I_{corr,f})/I_{corr,0}$$

3. Results

3.1. X-ray diffraction

The XRD patterns show that the phases obtained present well-crystallized structures of the LDH type (Fig. 2) [33,44,47–49]. The different spectra are indexed in an hexagonal lattice of rhombohedral symmetry (space group R $\bar{3}$m). The cell parameters were, as refined by the least square method, are given in table 2.

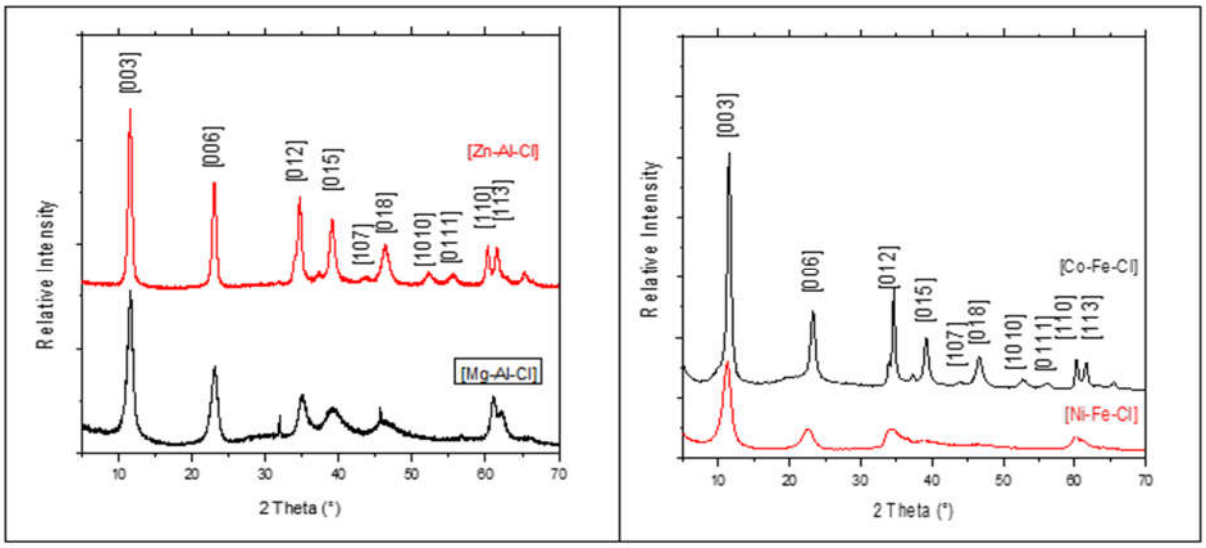

Figure 2. XRD patterns of (a) [Zn-Al-Cl], [Mg-Al-Cl] and (b) [Co-Fe-Cl] ,[Ni-Fe-Cl] phases.

Table 2. Cell parameters of [Zn-Al-Cl], [Mg-Al-Cl], [Ni-Fe-Cl], and [Co-Fe-Cl] LDHs.

Matrix	a (nm)	c (nm)
[Zn-Al-Cl]	0.307	2.321
[Mg-Al-Cl]	0.305	2.313
[Ni-Fe-Cl]	0.318	2.349
[Co-Fe-Cl]	0.309	2.301

Preprints (www.preprints.org) | NOT PEER-REVIEWED | Posted: 16 June 2023 doi:10.20944/preprints202306.1177.v1

3.2. Infrared spectroscopy

The four LDHs present FTIR features that are almost the same (Fig. 3)[50] . The broad and intense band at 3500 cm^{-1} is due to the elongation vibrations of O-H groups of the sheets and the interlayer water. The deformation vibrations of water molecules in the interlamellar space, $\delta(H_2O)$, are located around 1630 cm^{-1}. The band located around 1360 cm^{-1} is attributed to the valence vibration (ν_3) of carbonate ions, which indicates a slight contamination of the sample by atmospheric CO_2 during the elaboration of the solid materials. The M-O lattice vibrations (M = Zn, Mg, Co, Ni, Al, and Fe) in the sheets are observed at low wave numbers ($\nu < 830$ cm^{-1}) [51–53]. The bands located around 600 cm^{-1} correspond to the A_{2u} and E_u valence vibrations of M-O. The band at 430 cm^{-1} corresponds to the deformation vibrations of O-M-O. The presence of a shoulder around 830 cm^{-1} corresponds to the deformation vibration of hydroxyl groups, δ(OH).

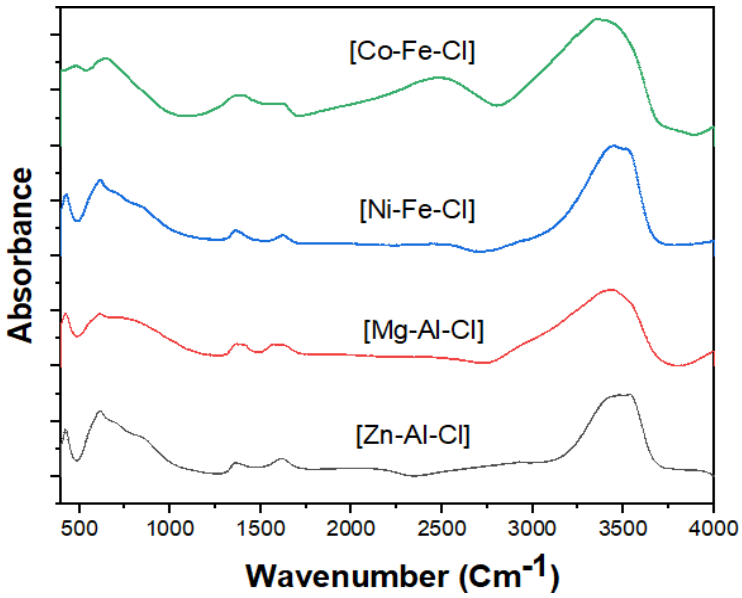

Figure 3. FTIR spectra of [Zn-Al-Cl], [Mg-Al-Cl], [Ni-Fe-Cl], and [Co-Fe-Cl] LDHs.

3.3. Thermal analyses

The thermogravimetry (TG) and differential TG (DTG) diagrams of the different LDH phases are presented in Figure 4. The mass losses and the DTG signals are summarized in Table 3 [54–56].

Table 3. TG and DTG diagrams of the four LDH phases

	Temperature (°C)	Mass loss (%)	DTG signal (°C)	Allocation
[Zn-Al-Cl]	25-200	21.0	140	Loss of physisorbed and interlayer water
	200-280	33.1	270	Dehydroxylation of LDH layers
	280-570	40.2	390	Loss of chloride ions in form of HCl gas
	> 570		630	Formation of ZnO and $ZnAl_2O_4$
[Mg-Al-Cl]	25-210	40.1	130	Loss of physisorbed and interlayer water
	210-380	25.1	205	Dehydroxylation of LDH layers
	380-670	10.2	310	Loss of chloride ions in form of HCl gas
	> 670		670	Formation of MgO and $MgAl_2O_4$
[Ni-Fe-Cl]	25-210	30.1	130	Loss of physisorbed and interlayer water
	210-350	20.1	200	Dehydroxylation of LDH layers

Preprints (www.preprints.org) | NOT PEER-REVIEWED | Posted: 16 June 2023 doi:10.20944/preprints202306.1177.v1

	350-710	10.3	310	Loss of chloride ions in form of HCl gas
	> 710		470-690	Formation of NiO and $NiFe_2O_4$
	25-180	19.2	140	Loss of physisorbed and interlayer water
[Co-Fe-Cl]	180-410	36.1	285	Dehydroxylation of LDH layers
	410-720	9.1	460	Loss of chloride ions in form of HCl gas
	> 570		550-630	Formation of CoO and $CoFe_2O_4$

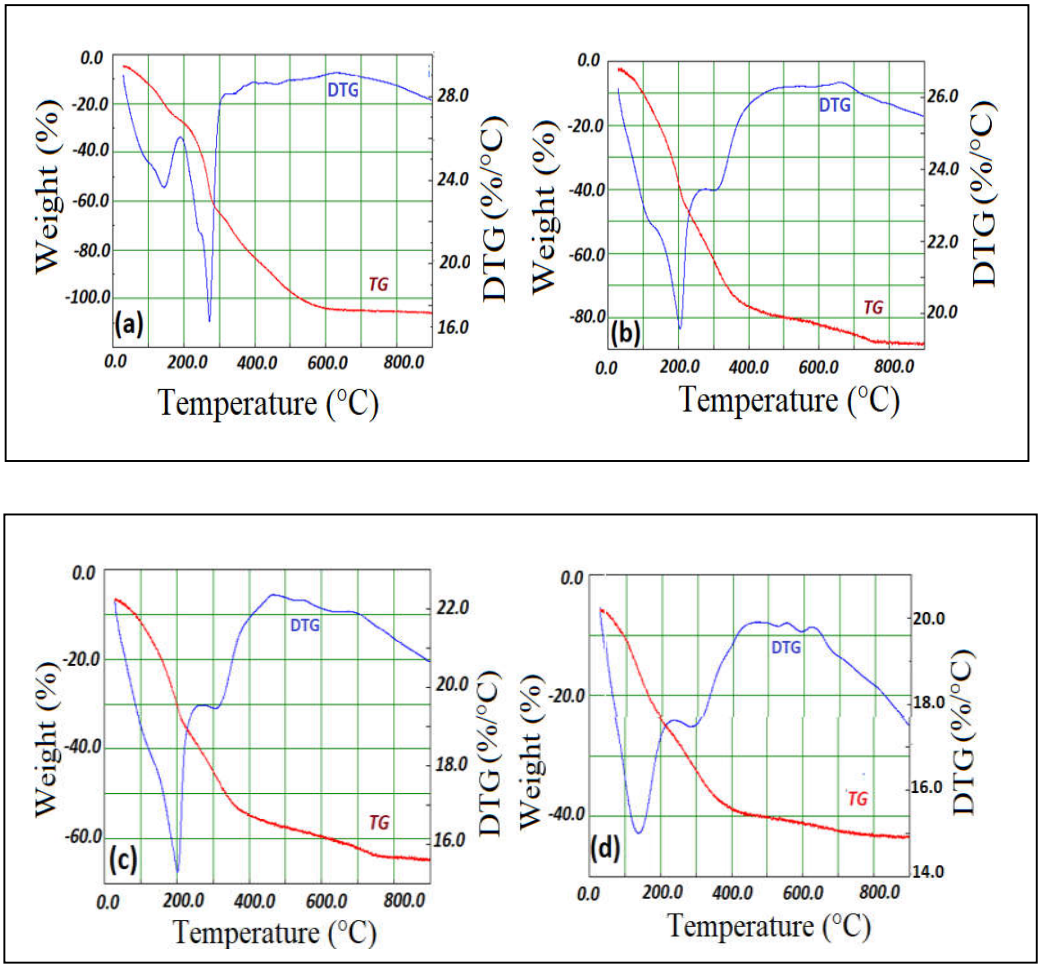

Figure 4. TG-DTG curves of (a) [Zn-Al-Cl], (b) [Mg-Al-Cl], (c) [Ni-Fe-Cl] and (d) [Co-Fe-Cl] LDHs.

3.4. Evaluation of inhibitory efficiency

3.4.1. Gravimetry

The gravimetric tests indicate that the mass loss, Δm, decreases when the LDH concentration increases from 0 $g.L^{-1}$ to 1.2 $g.L^{-1}$ (Table 4). This generates an increase in the inhibitory efficiency.

Preprints (www.preprints.org) | NOT PEER-REVIEWED | Posted: 16 June 2023 doi:10.20944/preprints202306.1177.v1

Table 4. Inhibitory efficiencies of the LDH-based solutions as determined by gravimetric tests (m_i and m_f are the masses of the steel before and after immersion in the solution, respectively).

[Zn-Al-Cl]			
C (g.L^{-1})	0	0.6	1.2
m_i (g)	3.468	3.145	3.591
m_f (g)	2.587	2.878	3.463
Δm (g)	0.881	0.267	0.128
EI (%)	-	69.69	85.47

[Mg-Al-Cl]			
C (g.L^{-1})	0	0.6	1.2
m_i (g)	3.162	4.122	3.947
m_f (g)	2.478	3.839	3.773
Δm (g)	0.684	0.273	0.174
EI (%)	-	60.08	74.56

[Ni-Fe-Cl]			
C (g.L^{-1})	0	0.6	1.2
m_i (g)	3.677	3.447	3.195
m_f (g)	3.059	3.234	3.104
Δm (g)	0.618	0.213	0.091
EI (%)	-	65.53	85.27

[Co-Fe-Cl]			
C (g.L^{-1})	0	0.6	1.2
m_i (g)	3.694	3.548	4.382
m_f (g)	2.921	3.246	4.12
Δm (g)	0.773	0.302	0.262
EI (%)	-	60.93	66.10

3.4.2. Voltammetry

The cathodic and anodic polarization curves of the steel in HCl, in the absence and presence of the LDH inhibitors, are presented in Figure 5.

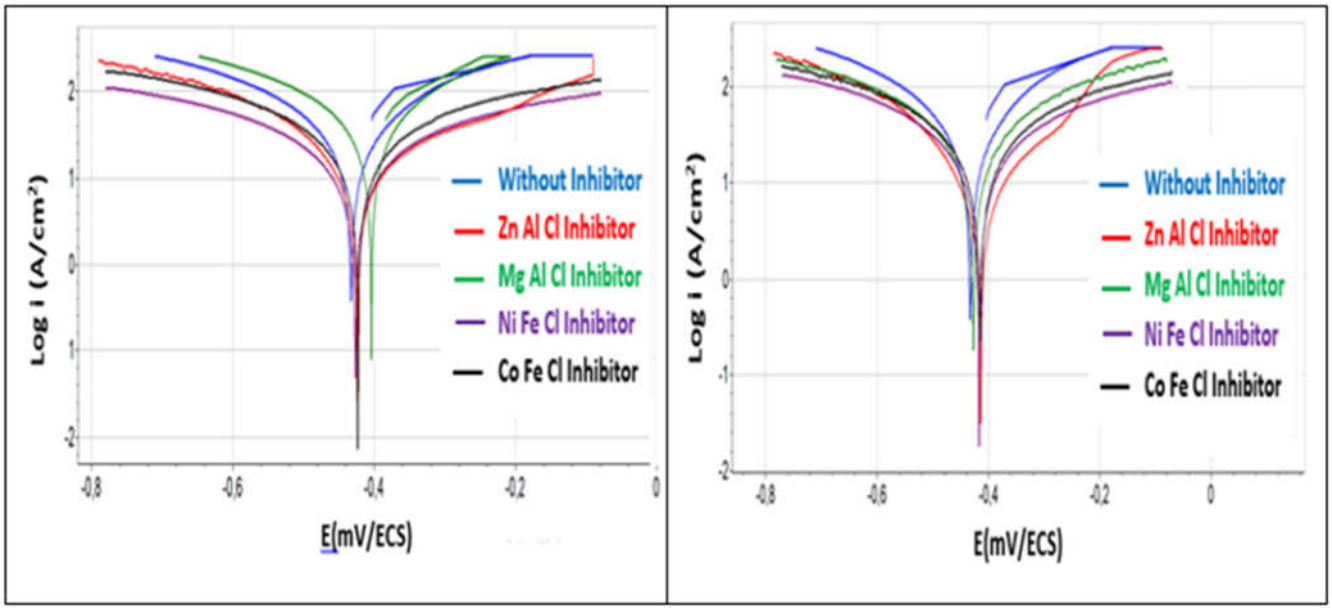

Figure 5. Polarization curves of steel in HCl without and with LDH inhibitors at the concentrations of (a) 0.6 g.L^{-1} and (b) 1.2 g.L^{-1}

Preprints (www.preprints.org) | NOT PEER-REVIEWED | Posted: 16 June 2023 doi:10.20944/preprints202306.1177.v1

The electrochemical parameters and inhibitory efficiencies (%) determined for the four LDH inhibitors are reported in Table 5. βa and βc are Tafel coefficients.

Table 5: Result of the inhibitory efficiencies of the [Zn-Al-Cl], [Mg-Al-Cl], [Ni-Fe-Cl], and [Co-Fe-Cl] inhibitors.

[Zn-Al-Cl]					
C ($g.L^{-1}$)	I_{corr} (mA/cm^2)	E (V)	βa (V)	βc (V)	Inhibitor efficiency (%)
0	15.58	- 0.432	0.125	0.132	--
0.6	04.58	- 0.423	0.100	0.079	70.58
1.2	02.55	- 0.414	0.073	0.066	83.65
[Mg-Al-Cl]					
C_{inh} ($g.L^{-1}$)	I_{corr} (mA/cm^2)	E (V)	βa (V)	βc (V)	Inhibitor efficiency (%)
0	15.58	-0.432	0.125	0.132	--
0.6	06.29	-0.404	0.040	0.040	59.62
1.2	03.94	-0.428	0.050	0.047	74.73
[Ni-Fe-Cl]					
C_{inh} ($g.L^{-1}$)	I_{corr} (mA/cm^2)	E (V)	βa (V)	βc (V)	Inhibitor efficiency (%)
0	15.58	-0.432	0.125	0.132	--
0.6	05.22	-0.425	0.109	0.114	66.46
1.2	02.59	-0.416	0.045	0.048	83.33
[Co-Fe-Cl]					
C_{inh} ($g.L^{-1}$)	I_{corr} (mA/cm^2)	E (V)	βa (V)	βc (V)	Inhibitor efficiency (%)
0	15.58	-0.432	0.125	0.132	--
0.6	06.18	-0.423	0.093	0.085	60.34
1.2	04.92	-0.416	0.072	0.068	68.38

A first analysis of these curves shows that the anodic and cathodic reactions are affected by the addition of the inhibitor. Indeed, the presence of the inhibitor at a 0.6 $g.L^{-1}$ concentration causes a shift of the corrosion potential to positive values. The addition of the inhibitor in the HCl solution induces the decrease of the anodic current corresponding to the attack of the metal and also the decrease of the cathodic current corresponding to the reduction of oxygen. In addition, the corrosion current density decreases significantly for all concentrations compared to that obtained without the inhibitor. It may be concluded that the inhibitors present a good inhibiting effect, which efficiency

Preprints (www.preprints.org) | NOT PEER-REVIEWED | Posted: 16 June 2023 doi:10.20944/preprints202306.1177.v1

increases with their increasing concentration. The steel protection may be due to the adsorption of the LDH ions on its surface, blocking thus its active sites.

The higher efficiency of [Zn-Al-Cl] compared to [Mg-Al-Cl] may be explained by the electronegativity and the van der Waals radii of the dominating metal cations of the LDH. Zn (0.65 and 0.139 nm), which is less electronegative and smaller than Mg (1.31 and 0.173 nm), may be more attracted by the steel. As a result, Zn will occupy more adsorption sites than Mg preventing thus more H^+ ions from HCl to reach the steel surface. This comparison is also valid for [Ni-Fe-Cl] and [Co-Fe-Cl] for which the metals have the following electronegativity and radii values, respectively: Ni (1.91 and 0.163 nm) and Co (1.88 and 0.200 nm) [57,58].

3.5. Surface analysis by optical microscopy, SEM, and EDS.

3.5.1. Optical microscopy

The optical microscopy images confirm the electrochemical results obtained (Fig. 6). A comparison between the surface of steel exposed to the HCl solution with and without HDL inhibitor shows that the localized corrosion is clearly diminished in the presence of the HDL inhibitor.

In the absence of the inhibitor, the steel surface presents rough and irregular features, in the form of cavities, cracks, and deposits, indicating that corrosion has occurred. Conversely, the steel surface is smoother in the presence of each of the four LDH inhibitors.

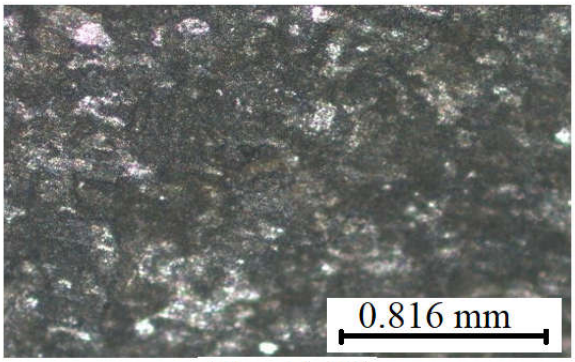

[Zn-Al-Cl]

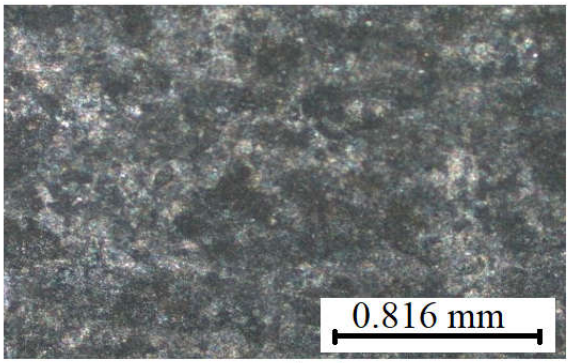

[Mg-Al-Cl]

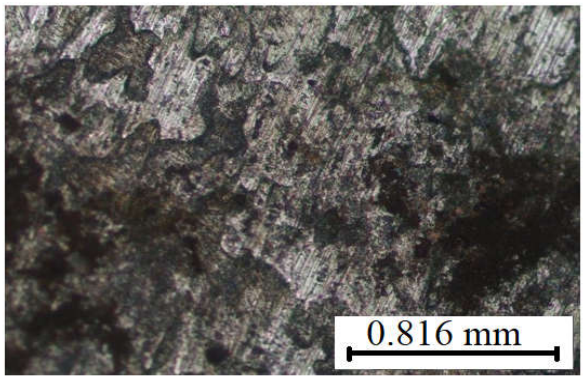

Without inhibitor

Preprints (www.preprints.org) | NOT PEER-REVIEWED | Posted: 16 June 2023 doi:10.20944/preprints202306.1177.v1

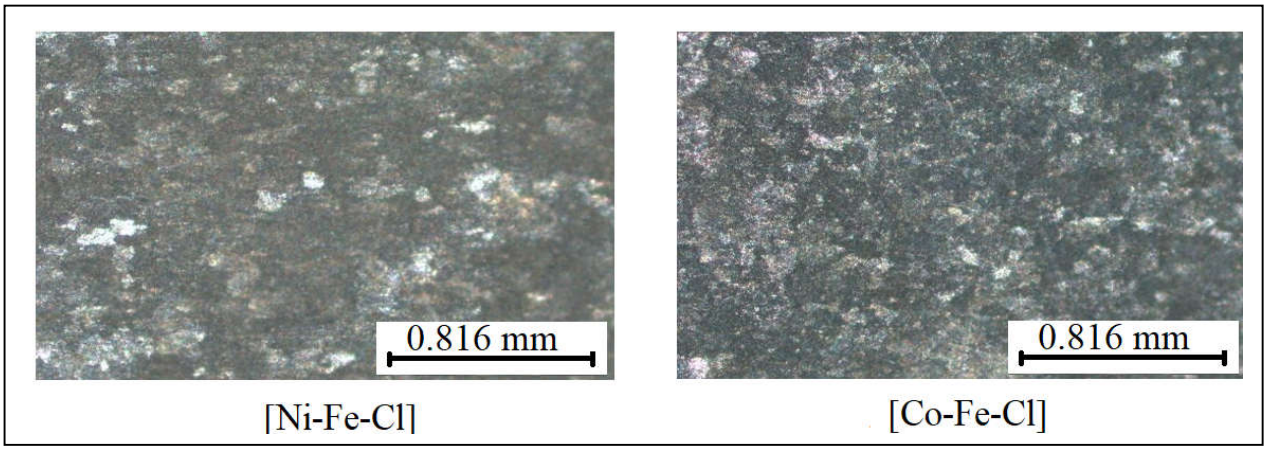

Figure 6. Optical microscope photographs of the mild steel surface after 10 min immersion in 18.5% HCl, in the absence and in the presence of 1.2 $g.L^{-1}$ LDH inhibitor.

3.5.2. Scanning electron microscopy

The SEM micrograph of the steel exposed to the HCl solution without LDH also shows the development of a thick layer of corrosion products. Indeed, this layer may be related to the formation of iron oxides. This layer presents a porous structure with pits and crevices that allow for H^+, Cl^- and water to diffuse into the steel leading to more deterioration of its structure.

On the other hand, images of the steel in the presence of the each of the four LDH inhibitors show a smoother and less weathered surface, indicating that corrosion was slowed or inhibited by the action of the inhibitor. This may be explained by the adsorption of the metal cations of the LDH inhibitors on the steel surface.

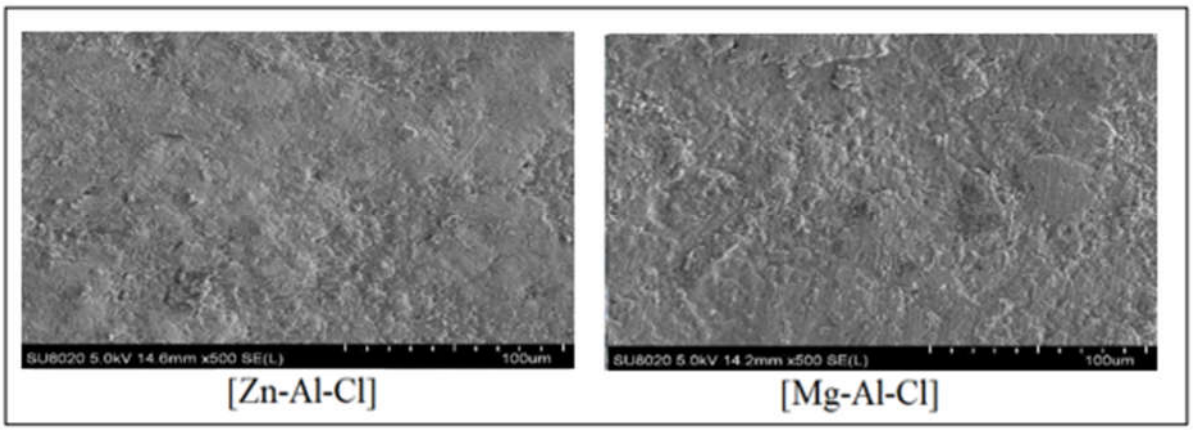

Preprints (www.preprints.org) | NOT PEER-REVIEWED | Posted: 16 June 2023 doi:10.20944/preprints202306.1177.v1

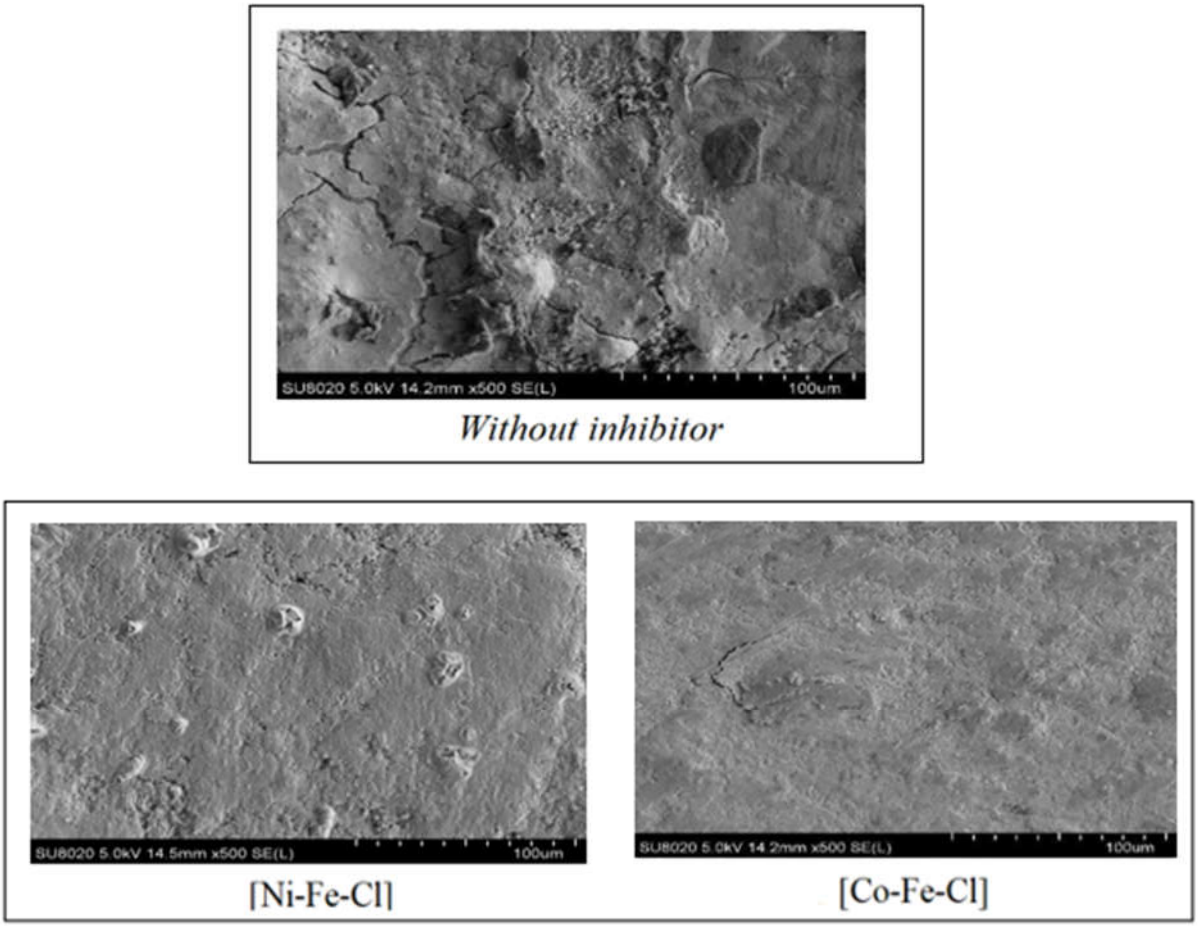

Figure 7. SEM micrographs of the mild steel surface after 10 min immersion in 18.5% HCl, in the absence and in the presence of 1.2 $g.L^{-1}$ LDH

3.5.3. Energy dispersive spectroscopy analysis

The EDS analyses of the surface of the steel exposed to the HCl-LDH solutions are presented in figure 8. Each of the four diagrams presents lines relative to the ions present in the corresponding LDH. The inhibition process of the LDH may have started with an adsoption of the cations from the dissolved LDH. The repulsive interactions between H^+ ions and the LDH metal cations adsorbed on the steel surface, in the HCl solution, allowed to protect the steel. These metal cations may have been deposited on the steel surface in form of metal oxides

Preprints (www.preprints.org) | NOT PEER-REVIEWED | Posted: 16 June 2023 doi:10.20944/preprints202306.1177.v1

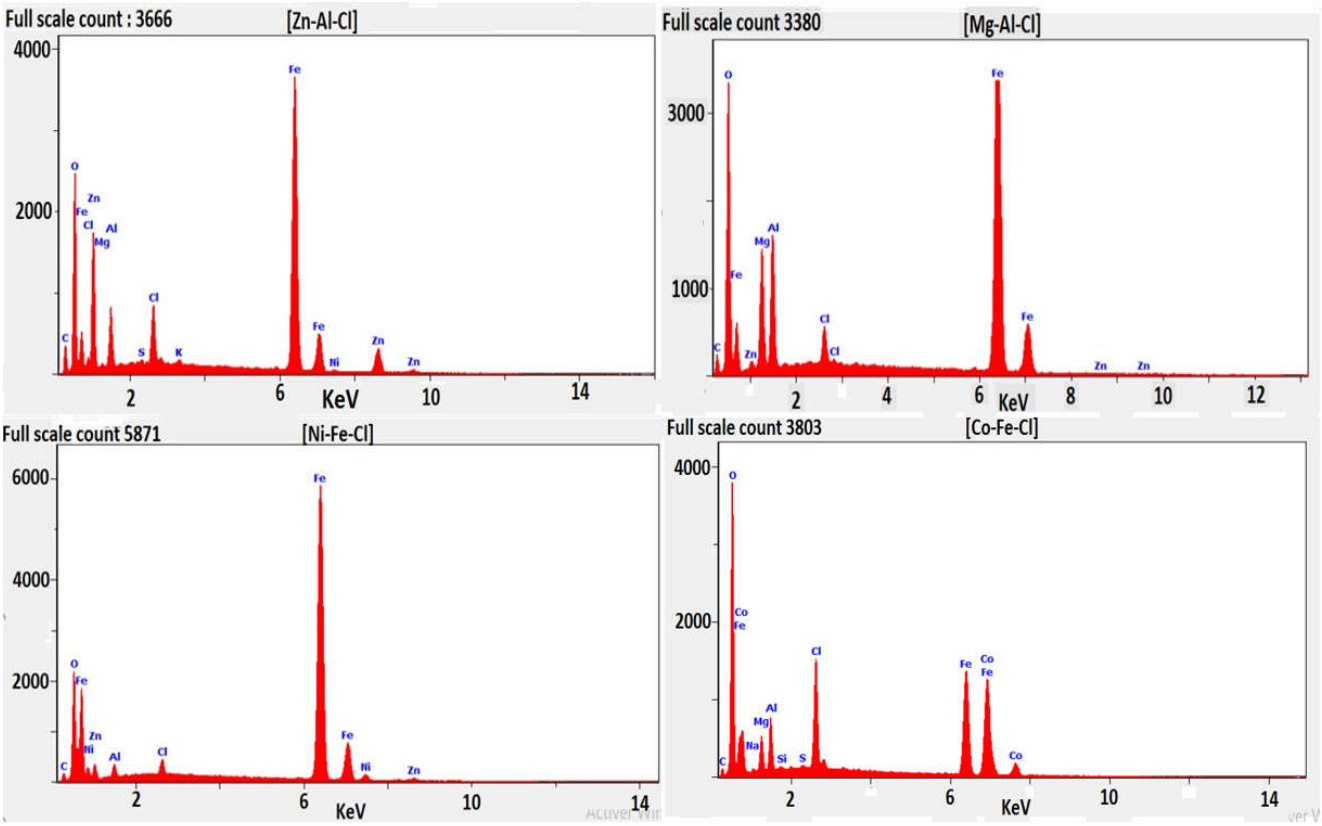

Figure 8. *EDS analysis of the surface of the steel exposed to the HCl-LDH solutions*

4. Conclusions

The present work was devoted to the study of the improvement of the electrochemical corrosion resistance of mild steel in a concentrated HCl solution by the use of [Zn-Al-Cl], [Mg- Al-Cl], [Ni-Fe-Cl], and [Co-Fe-Cl] HDLs as inhibitors.

The LDH materials were prepared by coprecipitation and characterized by XRD, FTIR, and thermal analyses.

This study of the inhibitory efficiency was carried out by gravimetric and electrochemical methods (polarization curves). The results obtained show that all the four LDHs used have acted as corrosion inhibitors of the steel in the HCl aggressive environment. The results may be summarized as follows.

- The best effect is observed with the maximum LDH concentration of 1.2 $g.L^{-1}$ using [Zn-Al-Cl] and [Ni-Fe-Cl] LDHs which inhibitory efficiency reached 83.65% and 83.33%, respectively.
- The displacement of the free potentials towards more anodic values characterizes the formation of a protective layer of the LDHs on the steel surface.
- Increasing the concentration of each of the four inhibitors decreases the corrosion current densities, thus the corrosion rates, especially in the cases of [Zn-Al-Cl] and [Ni-Fe-Cl].
- The surface morphology analyses of the steel after chemical pickling in HCl in the absence of inhibitor allowed to identify the type of corrosion (pitting corrosion) and the damaged state (cracks). These undesirable effects were absent in the presence of the inhibitors, indicating a good protection of the steel against corrosion.
- "The same solutions containing the corrosion inhibitor can be used multiple times for different metal plates."

The main outcome of this work is that the fight against corrosion of steel in a HCl environment is possible using a new generation of inhibitors that have the advantage of being easier to obtain and less toxic than the traditional inhibitors.

References

1. El Ashry, E.S.; El Nemr, A.; Essawy, S.; Ragab, S. Corrosion Inhibitors - Part II: Quantum Chemical Studies on the Corrosion Inhibitions of Steel in Acidic Medium by Some Triazole, Oxadiazole and Thiadiazole Derivatives. *Electrochimica Acta* **2006**, *51*, 3957–3968, doi:10.1016/j.electacta.2005.11.010.
2. Anionic Oxide-vanadium Schiff Base Amino Acid Complexes as Potent Inhibitors and as Effective Catalysts for Sulfides Oxidation: Experimental Studies Complemented with Quantum Chemical Calculations - ScienceDirect Available online: https://www.sciencedirect.com/science/article/pii/S0167732217345488?casa_token=IZVOSHcKv0gAAAAA:ZHzIeesCXVgE1V1nQuRldrLh7HtIj7QKNqlv1vEee2POeuuHRVlwE1-gl7x2JGMhPxZD8_zOyA (accessed on 8 June 2023).
3. Zhang, B.; He, C.; Chen, X.; Tian, Z.; Li, F. The Synergistic Effect of Polyamidoamine Dendrimers and Sodium Silicate on the Corrosion of Carbon Steel in Soft Water. *Corrosion Science* **2015**, *90*, 585–596, doi:10.1016/j.corsci.2014.10.054.
4. Synthesis of Polar Unique 3d Metal-Imine Complexes of Salicylidene Anthranilate Sodium Salt. Homogeneous Catalytic and Corrosion Inhibition Performance - ScienceDirect Available online: https://www.sciencedirect.com/science/article/pii/S1876107018302359?casa_token=sq1Q0ndJ3F0AAAAA:fSTEeWIJ4XWSqTGnblXCpQ_OMxQJFjLY2p54Zncv9P1CVFU7h8GwztpC-ifJbwo3JonWJBMuGA (accessed on 8 June 2023).
5. Experimental Investigation of Newly Synthesized Gemini Cationic Surfactants as Corrosion Inhibitors of Mild Steel in 1.0 M HCl | SpringerLink Available online: https://link.springer.com/article/10.1134/S2070205118010173 (accessed on 8 June 2023).
6. Egyptian Petroleum Research Institute (EPRI), Nasr City, Cairo, Egypt; A. Hegazy, M. Corrosion Inhibition Performance of a Novel Cationic Surfactant for Protection of Carbon Steel Pipeline in Acidic Media. *Int. J. Electrochem. Sci.* **2018**, 6824–6842, doi:10.20964/2018.07.53.
7. Corrosion Inhibition Behavior of Indazole Derivative as a Green Corrosion Inhibitor for Mild Steel in Hydrochloric Acid: Electrochemical, Weight Loss and DFT Simulations Studies | Chahdi, H. Steli, C. Ad, Y. Ouzidan, E. M. Essassi, A. Chetouani, B. Hammouti | Moroccan Journal of Chemistry Available online: https://revues.imist.ma/index.php/morjchem/article/view/11041 (accessed on 8 June 2023).
8. Al-Taweel, S.; Al-Janabi, K.; Luaibi, H.; Al-Amiery, A.; Gaaz, T. Evaluation and Characterization of the Symbiotic Effect of Benzylidene Derivative with Titanium Dioxide Nanoparticles on the Inhibition of the Chemical Corrosion of Mild Steel. *International Journal of Corrosion and Scale Inhibition* **2019**, *8*, 1149–1169, doi:10.17675/2305-6894-2019-8-4-21.
9. Synergistic of a Coumarin Derivative with Potassium Iodide on the Corrosion Inhibition of Aluminum Alloy in 1.0 M H2SO4 | SpringerLink Available online: https://link.springer.com/article/10.1007/s12540-014-3008-3 (accessed on 8 June 2023).
10. Effect of 1,3,4-Thiadiazole Scaffold on the Corrosion Inhibition of Mild Steel in Acidic Medium: An Experimental and Computational Study | SpringerLink Available online: https://link.springer.com/article/10.1007/s40735-019-0243-7 (accessed on 8 June 2023).
11. Experimental and Computational Investigation on the Corrosion Inhibition Characteristics of Mild Steel by Some Novel Synthesized Imines in Hydrochloric Acid Solutions - ScienceDirect Available online: https://www.sciencedirect.com/science/article/pii/S0010938X14005617?casa_token=lOzkxqmREXwAAAAA:Bz75m6r6vSOszxkK5ye5C7t76gSTa8ojor-dMAccEHlMil2aW-N643Holk9lAwmwHf0mCZbzcA (accessed on 8 June 2023).
12. Muthukumar, N. Chapter 21 - Petroleum Products Transporting Pipeline Corrosion—A Review. In *The Role of Colloidal Systems in Environmental Protection*; Fanun, M., Ed.; Elsevier: Amsterdam, 2014; pp. 527–571 ISBN 978-0-444-63283-8.
13. Bai, Y.; Bai, Q. Subsea Corrosion and Scale. *Subsea Engineering Handbook, 2nd ed.; Gulf Professional Publishing: Oxford, UK* **2019**, 455–487.
14. Arya, S.B.; Joseph, F.J. Chapter 3 - Electrochemical Methods in Tribocorrosion. In *Tribocorrosion*; Siddaiah, A., Ramachandran, R., Menezes, P.L., Eds.; Academic Press, 2021; pp. 43–77 ISBN 978-0-12-818916-0.
15. Murariu, M.; Oancea, A.-V.; Ursu, C.; Rusu, B.G.; Cotofana, C.; Simionescu, B.; Olaru, M. Chapter 20 - Surface Properties of POSS Nanocomposites. In *Polyhedral Oligomeric Silsesquioxane (POSS) Polymer Nanocomposites*; Thomas, S., Somasekharan, L., Eds.; Elsevier, 2021; pp. 421–448 ISBN 978-0-12-821347-6.
16. Norman, E.H. NACE Glossary of Corrosion Terms. *Materials Protection* **1965**, *4*, 79.

17. Study by Acoustic Emission and Electrochemical Methods of the..|INIS Available online: https://inis.iaea.org/search/search.aspx?orig_q=RN:36034413 (accessed on 8 June 2023).
18. Corrosion and Anticorrosion. Industrial Practice|INIS Available online: https://inis.iaea.org/search/search.aspx?orig_q=RN:33045680 (accessed on 8 June 2023).
19. Development of a Predictive Model for Corrosion Inhibition of Carbon Steel by Imidazole and Benzimidazole Derivatives - ScienceDirect Available online: https://www.sciencedirect.com/science/article/pii/S0010938X16300798?casa_token=zEaB5l6WGxoAAAAA:QZodXnBZNaWr5OFrbcDdiLHWJVg2hrtDr1zs1TkppjfXzdc9MWcR-EOjw92iEK501_W6gw0vBw (accessed on 8 June 2023).
20. School of Chemistry and Chemical Engineering, Chongqing University, Chongqing 400044, P.R. China; Luo, L. Study on 1-Allyl-3-Butylimidazalium Bromine as Corrosion Inhibitor for X65 Steel in 0.5 M H2SO4 Solution. *Int. J. Electrochem. Sci.* **2016**, 8177–8192, doi:10.20964/2016.10.52.
21. Hamner, N.E. Scope and Importance of Inhibitor Technology. *Corrosion Inhibitors, Houston, NACE* **1994**.
22. COROZIUNEA MATERIALELOR METALICE - S.ZAMFIR, R. VIDU SI V. BRINZOI Available online: https://www.galeriile-cismigiu.ro/coroziunea-materialelor-metalice-szamfir-r-vidu-si-v-brinzoi-p26618 (accessed on 8 June 2023).
23. Molybdate and Tungstate as Corrosion Inhibitors for Cold Rolling Steel in Hydrochloric Acid Solution - ScienceDirect Available online: https://www.sciencedirect.com/science/article/pii/S0010938X05000521?casa_token=ScW1ATJ62SIAAAAA:-A-4H9dTGAEaeWkT_HkF49IZlgOiG_EpPlqkGvm1_Z7RtAN3cJRpvioF6gmB8sDxXXaaFkNlxw (accessed on 8 June 2023).
24. Effects of Chromate and Chromate Conversion Coatings on Corrosion of Aluminum Alloy 2024-T3 - ScienceDirect Available online: https://www.sciencedirect.com/science/article/abs/pii/S0257897201010039 (accessed on 8 June 2023).
25. Bastos, A.C.; Zheludkevich, M.L.; Ferreira, M.G.S. A SVET Investigation on the Modification of Zinc Dust Reactivity. *Progress in Organic Coatings* **2008**, *63*, 282–290, doi:10.1016/j.porgcoat.2008.01.013.
26. Effect of Various Cations on the Formation of Calcium Carbonate and Barium Sulfate Scale with and without Scale Inhibitors | Industrial & Engineering Chemistry Research Available online: https://pubs.acs.org/doi/abs/10.1021/ie2003494 (accessed on 8 June 2023).
27. Corrosion Inhibition of AA2024-T3 By Sodium Silicate | Request PDF Available online: https://www.researchgate.net/publication/261139143_Corrosion_Inhibition_of_AA2024-T3_By_Sodium_Silicate (accessed on 8 June 2023).
28. Yohai, L.; Vázquez, M.; Valcarce, M.B. Phosphate Ions as Corrosion Inhibitors for Reinforcement Steel in Chloride-Rich Environments. *Electrochimica Acta* **2013**, *102*, 88–96, doi:10.1016/j.electacta.2013.03.180.
29. Lafont, M.C.; Pebere, N.; Moran, F.; Bleriot, P. Inhibition de La Corrosion d'un Acier Au Carbone Par Des Produits Dérivés de Phosphonates En Association Avec Des Sels de Zinc. *rseau* **2005**, *6*, 97–112, doi:10.7202/705168ar.
30. Bensaada, S.; Bouziane, M.T.; Mohammedi, F.; Zergui, B.; Bouras, A. EFFET DES INHIBITEURS DE CORROSION ZnCl2, Na2MoO4 ET ZnCl2 +Na2MoO4 SUR LE COMPORTEMENT DE L'ACIER POUR ARMATURE A BETON EN MILIEU OXYDANT NaCl. *LARHYSS Journal P-ISSN 1112-3680 / E-ISSN 2521-9782* **2013**.
31. Quantum Chemical Studies of Some Rhodanine Azosulpha Drugs as Corrosion Inhibitors for Mild Steel in Acidic Medium - Ebenso - 2010 - International Journal of Quantum Chemistry - Wiley Online Library Available online: https://onlinelibrary.wiley.com/doi/abs/10.1002/qua.22249 (accessed on 8 June 2023).
32. Pillaring of Layered Double Hydroxides (LDH's) by Polyoxometalate Anions | Journal of the American Chemical Society Available online: https://pubs.acs.org/doi/pdf/10.1021/ja00219a048 (accessed on 8 June 2023).
33. Cavani, F.; Trifirò, F.; Vaccari, A. Hydrotalcite-Type Anionic Clays: Preparation, Properties and Applications. *Catalysis Today* **1991**, *11*, 173–301, doi:10.1016/0920-5861(91)80068-K.
34. Playle, A.C.; Gunning, S.R.; Llewellyn, A.F. The in Vitro Antacid and Anti-Pepsin Activity of Hydrotalcite. *Pharm Acta Helv* **1974**, *49*, 298–302.
35. Mishra, G.; Dash, B.; Pandey, S. Layered Double Hydroxides: A Brief Review from Fundamentals to Application as Evolving Biomaterials. *Applied Clay Science* **2018**, *153*, 172–186, doi:10.1016/j.clay.2017.12.021.

36. Mousty, C.; Therias, S.; Forano, C.; Besse, J.-P. Anion-Exchanging Clay-Modified Electrodes: Synthetic Layered Double Hydroxides Intercalated with Electroactive Organic Anions. *Journal of Electroanalytical Chemistry* **1994**, *374*, 63–69, doi:10.1016/0022-0728(94)03346-3.
37. Badreddine, M.; Khaldi, M.; Legrouri, A.; Barroug, A.; Chaouch, M.; De Roy, A.; Besse, J.P. Chloride-Hydrogenophosphate Ion Exchange into the Zinc–Aluminium–Chloride Layered Double Hydroxide. *Materials Chemistry and Physics* **1998**, *52*, 235–239, doi:10.1016/S0254-0584(97)02050-6.
38. Ookubo, A.; Ooi, K.; Hayashi, H. Hydrotalcites as Potential Adsorbents of Intestinal Phosphate. *J Pharm Sci* **1992**, *81*, 1139–1140, doi:10.1002/jps.2600811120.
39. Buchheit, R.G.; Guan, H.; Mahajanam, S.; Wong, F. Active Corrosion Protection and Corrosion Sensing in Chromate-Free Organic Coatings. *Progress in Organic Coatings* **2003**, *47*, 174–182, doi:10.1016/j.porgcoat.2003.08.003.
40. Characterization of Inhibitor Release from Zn-Al-[V10O28]6− Hydrotalcite Pigments and Corrosion Protection from Hydrotalcite-Pigmented Epoxy Coatings | CORROSION Available online: https://meridian.allenpress.com/corrosion/article-abstract/64/3/230/162739/Characterization-of-Inhibitor-Release-from-Zn-Al (accessed on 8 June 2023).
41. Formation of Mg,Al-Hydrotalcite Conversion Coating on Mg Alloy in Aqueous HCO3−/CO32− and Corresponding Protection against Corrosion by the Coating - ScienceDirect Available online: https://www.sciencedirect.com/science/article/pii/S0010938X09000535?casa_token=nrOuPpnd3N0AAAAA:OpkLPTiwcx7FLFfMci1AhGfkjEp7dlIEM_ey2WTox-nBpSm0KsmMRMYeNsxEl0aSzjnBZUPH79M (accessed on 9 June 2023).
42. Jing, C.; Dong, B.; Raza, A.; Zhang, T.; Zhang, Y. Corrosion Inhibition of Layered Double Hydroxides for Metal-Based Systems. *Nano Materials Science* **2021**, *3*, 47–67, doi:10.1016/j.nanoms.2020.12.001.
43. Gastuche, M.C.; Brown, G.; Mortland, M.M. Mixed Magnesium-Aluminiun Hydroxides. I. Preparation and Characterization of Compounds Formed in Dialysed Systems. *Clay Minerals* **1967**, *7*, 177–192, doi:10.1180/claymin.1967.007.2.05.
44. Miyata, S. The Syntheses of Hydrotalcite-Like Compounds and Their Structures and Physico-Chemical Properties—I: The Systems Mg2+-Al3+-NO3−, Mg2+-Al3+-Cl−, Mg2+-Al3+-ClO4−, Ni2+-Al3+-Cl− and Zn2+-Al3+-Cl−. *Clays Clay Miner.* **1975**, *23*, 369–375, doi:10.1346/CCMN.1975.0230508.
45. Legrouri, A.; Badreddine, M.; Barroug, A. Influence of PH on the Synthesis of the Zn–Al–Nitrate Layered Double Hydroxide and the Exchange of Nitrate by Phosphate Ions.
46. Khaldi, M.; Badreddine, M.; Legrouri, A.; Chaouch, M.; Barroug, A.; De Roy, A.; Besse, J.P. Preparation of a Well-Ordered Layered Nanocomposite from Zinc–Aluminum–Chloride Layered Double Hydroxide and Hydrogenophosphate by Ion Exchange. *Materials Research Bulletin* **1998**, *33*, 1835–1843, doi:10.1016/S0025-5408(98)00185-8.
47. Synthesis and Characterization of Intercalated Layered Double Metal Hydroxides With Interlayer Aromatic Molecular Anions: Intercalation of 9,10-Anthraquinonedisulfonates Between Layers of Mg and Al Layered Double Hydroxides(MgAl-LDH): Molecular Crystals and Liquid Crystals Science and Technology. Section A. Molecular Crystals and Liquid Crystals: Vol 286, No 1 Available online: https://www.tandfonline.com/doi/abs/10.1080/10587259608042280 (accessed on 8 June 2023).
48. Badreddine, M.; Legrouri, A.; Barroug, A.; De Roy, A.; Besse, J.-P. Influence of PH on Phosphate Intercalation in Zinc-Aluminum Layered Double Hydroxide. *Collect. Czech. Chem. Commun.* **1998**, *63*, 741–748, doi:10.1135/cccc19980741.
49. Newman, S.P.; Jones, W. Synthesis, Characterization and Applications of Layered Double Hydroxides Containing Organic Guests. *New J. Chem.* **1998**, *22*, 105–115, doi:10.1039/A708319J.
50. Bonnet, S. Synthese et Caracterisation de Materiaux Hybrides de Type Hdl-Porphyrine. These de doctorat, Clermont-Ferrand 2, 1997.
51. Microwave-Assisted Reconstruction of Ni,Al Hydrotalcite-like Compounds - ScienceDirect Available online: https://www.sciencedirect.com/science/article/pii/S0022459608000856?casa_token=flo2t0p-gtgAAAAA:sNmk4tqI-YywIbFUK-ozWRHod497kkZHsxJk27YYvjSf6Oydh9nY5PCDUj2Ve1qCDNscxsSqrWI (accessed on 8 June 2023).
52. Gimbert, F.; Morin-Crini, N.; Renault, F.; Badot, P.-M.; Crini, G. Adsorption Isotherm Models for Dye Removal by Cationized Starch-Based Material in a Single Component System: Error Analysis. *Journal of Hazardous Materials* **2008**, *157*, 34–46, doi:10.1016/j.jhazmat.2007.12.072.
53. del Arco, M.; Malet, P.; Trujillano, R.; Rives, V. Synthesis and Characterization of Hydrotalcites Containing Ni(II) and Fe(III) and Their Calcination Products. *Chem. Mater.* **1999**, *11*, 624–633, doi:10.1021/cm9804923.

54. Stählin, W.; Oswald, H.R. The Infrared Spectrum and Thermal Analysis of Zinc Hydroxide Nitrate. *Journal of Solid State Chemistry* **1971**, *3*, 252–255, doi:10.1016/0022-4596(71)90037-5.
55. Morpurgo, S.; Lo Jacono, M.; Porta, P. Copper—Zinc—Cobalt—Chromium Hydroxycarbonates and Oxides. *Journal of Solid State Chemistry* **1995**, *119*, 246–253, doi:10.1016/0022-4596(95)80038-Q.
56. Khan, A.I.; Williams, G.R.; Hu, G.; Rees, N.H.; O'Hare, D. The Intercalation of Bicyclic and Tricyclic Carboxylates into Layered Double Hydroxides. *Journal of Solid State Chemistry* **2010**, *183*, 2877–2885, doi:10.1016/j.jssc.2010.09.036.
57. PAHO-Water Treatment: Principles and Design; Water Treatment: Principles and Design Available online: https://bases.bireme.br/cgi-bin/wxislind.exe/iah/online/?IsisScript=iah/iah.xis&src=google&base=PAHO&lang=p&nextAction=lnk&exprSearch=577&indexSearch=ID (accessed on 8 June 2023).
58. Suzuki, M. *Adsorption Engineering*; Chemical engineering monographs; Kodansha ; Elsevier: Tokyo : Amsterdam ; New York, 1990; ISBN 978-0-444-98802-7.